www.amlett.com, www.vbripress.com/aml, DOI: 10.5185/amlett.2015.5946 Published online by the VBRI Press in 2015

Tannic acid: A natural source to tailor nano crystalline silver particles of different morphologies as antibacterial agent

Henam Premananda Singh[1], Sarbjeet Singh Gujral[2], Surinder Kumar Sharma[2], Rakesh Kumar Sharma[1*]

[1]*Nanotechnology and Drug Delivery Research Lab, Department of Chemistry, University of Delhi, Delhi 110007, India*
[2]*Maharaja Surajmal Institute of Pharmacy, Janak Puri, New Delhi 110058, India*

[*]Corresponding author. Tel: (+91) 93100-50453; E-mail: sharmark101@yahoo.com

Received: 21 July 2015, Revised: 31 October 2015 and Accepted: 08 November 2015

ABSTRACT

In this work we have successfully prepared spherical and chain type silver nanoparticles of excellent size's homogeneity, reproducibility and stability using tannic acid. The synthesized nanometallic structures were characterized for their shape, size, thermal stability and crystalline nature. The mechanism for the formation of Ag NPs and shape evolution of the chain structure has been vividly explained. Further, these NPs were found to exhibit significant antibacterial activity against gram negative *Escherichia coli* bacteria but to different extend indicating the influence of particles morphology on their antibacterial behaviours. Copyright © 2015 VBRI Press.

Keywords: Bio-synthesis; tannic acid; silver nanoparticles; spherical chain; antibacterial activity.

Introduction

From the past few decades, there is a continuous permeate of nanotechnology among the scientific community. Nanoparticles (NPs) are currently the subject of intense investigation and research in this area are progressively made from a variety of viewpoints. They show unusual and fascinating behaviours with various applications over their bulk counterpart **[1, 2]**. Several chemical, physical, biological, and hybrid methods are well documented for the generation of NPs of different morphologies **[3-5]**. The development of biogenic routes for the fabrication of nanoparticles have gained immense interest owing to the growing need for development of environmentally benign technologies, their high atom economy, simplicity for the experimental procedures and versatility. In recent years, nano-scale metal synthesis using phytochemicals present in plant extracts of leaves, tuber, bark and buds have received more attention than chemical and physical methods, and even than the use of microbes due to the absence of any requirement to maintain an aseptic environment **[6-9]**. Plants can, therefore, be used as an alternative trigger for the green aqueous synthesis of nanomaterials. Tannic acid (TA) has been studied extensively for its antioxidant properties, as a chelating agent for several inorganic cations and has been used for the biomimetic growth of inorganic NPs **[10]**. A precise control over the size and shape of nano crystalline materials is a key issue. Therefore, presence of stabilizers and various surfactants is desirable to have a control over the growth of particles. Nano scale inorganic individual or composite particles that are either functionalized or not display unique physical and chemical properties; they represent an increasingly important material in the development of novel nanodevices which can be used in numerous physical, industrial, biological, biomedical, and pharmaceutical realms **[11-13]**. The increase resistance of microbes (bacteria.) against (bactericides) drugs, antibiotics (due to the development of resistant strains) and also high cost of treatment markedly need to formulate new types of effective, safe and cost effective innovative biocidal (antibacterial agent) materials. Recently, nano dimensional materials have emerged as novel antimicrobial (bacterial) agent as a consequence of their large surface to volume ratio providing more surface atoms than their bulk materials leading to a greater tendency of interaction with microbes. In fact there has been a great deal of interest surrounding the discovery that Ag NPs are significantly more effective antimicrobial agents in terms of the minimum effective concentration than their Ag^+ counterparts **[10, 14]**. Microbes are unlikely to develop resistance against silver, as they do against conventional and narrow-target antibiotics, because the metal attacks a broad range of targets in the organisms, which means that they would have to develop a host of mutations simultaneously to protect themselves **[15, 16]**. When Moyer **[17]** introduced the use of 0.5 % silver nitrate, in the 1960s, for the treatment of burns Ag came into picture. He proposed that this solution does not interfere with epidermal proliferation and possess antibacterial property against *Staphylococcus aureus*,

Pseudomonas aeruginosa and *Escherichia coli*. Ag NPs have the potential to act as an effective growth inhibitor against various microorganisms which makes it capable of being applied in diverse areas of medicine for antimicrobial control. As a consequence of this antimicrobial behaviour their incorporation into medical devices, tissues and other health related products promote higher preventive infection control. Though antimicrobial activity of Ag NPs has been established by past studies, the mode of action still remains unclear. Researchers predict that Ag species have an effect at the molecular, metabolic or membrane level of the microorganism **[18]**. Elechiguerra *et al.* found that Ag NPs undergo a size dependent interaction with human immune deficiency virus type 1, preferably via binding to gp120 glycoprotein knobs. The size-dependent interaction of Ag NPs with gram-negative bacteria has also been reported by the same group **[19]**. However, there is a little or less knowledge about the change in biological activity of Ag NPs along with the variation in the shape of the particles. In this work we have addressed briefly a simple, elegant and reproducible method for the preparation of Ag NPs of different morphologies with high atom economy utilizing TA as reducing agent as well as stabilizing agent. The particles were tailored at room temperature and in aqueous medium without using harmful chemicals following the basic principles of green chemistry, so the entire synthetic process remains as green approach. The particles after extraction from the reaction mixture were characterized and then the shape dependent antibacterial behaviour of these ensuing Ag NPs had been assayed onto multi drug resistance bacteria such *Escherichia coli* (E. coli).

Experimental

Material synthesis

All the chemicals used were of AR grade and they were utilized as such without any further purification. Purified sodium hydroxide (NaOH) pallets and pure silver nitrate ($AgNO_3$) were purchased from Merck. Tannic acid (TA) was obtained from Thomas Baker. Moreover glucose, Na_2HPO_4, KH_2PO_4, NH_4Cl, NaCl, $MgSO_4$, $CaCl_2$ and agar-agar were all obtained from central drug house (CDH), India. Folin & Ciocalteu's Phenol (FCP) reagent was bought from SRL Pvt. Ltd. The microbial strains was purchased from Microbial type culture collection and gene bank (MTCC) Chandigarh, India as freeze dried form. All the solutions were prepared in double distilled water (DDW).

Equipment

All were recorded in. To measure the UV-vis absorption spectrum the solution was taken in a 3.5 mL capacity quartz cuvette placed in a sample holder maintained at room temperature and scanned in the range of 300–700 nm.

Synthesis of nanoscale Ag particles – a green aqueous approach

We have prepared Ag NPs of different morphologies in a simple, fashionable manner by adding 250 µl of 2 % (w/v) freshly prepared $AgNO_3$ solution to a solution containing 9.88 ml of TA ($1x\ 10^{-3}$ M) and 120 µl of NaOH (0.2 M) at room temperature. Initially for the first sample, the solution was stirred moderately in a continuous manner for 30 minutes. And for the second sample, the reaction system was stirred uniformly for 24 hrs. Such tuning of stirring period leads to variation particle morphology. The so-synthesis particles were sonicated, centrifuged and washed with DDW thoroughly for three times. The particles were finally collected and dispersed in 1 ml of DDW. These synthesized Ag NPs were characterized for their shape, size, crystalline nature, by using TEM (TECNAI G^2 200 KV instrument), XRD (Rigaku miniflex desktop), FT-IR (Spectrum BX FTIR, Perkin Elmer), TGA (Perkin Elmer DTA/TGA/DSC instrument) and UV-vis spectra (UV-vis spectrophotometer-1601, Shimadzu). The XRD radiation was CuKα of 0.154 nm wavelength and scanned in the 2Θ range of $20\text{-}90^0$. The FT-IR spectra were taken in the range 400-4000 cm^{-1}. And UV-vis scan was performed between wavelengths of 300 nm and 700 nm.

Qualitative spectrophotometric assay of TA

The synthesized Ag NPs were submitted to Folin-Ciocalteu method for qualitative spectrophotometric determination of TA present along with the metal particles. The standard solution was prepared by taking 17 mg of TA and 150 µl of NaOH (0.2 M) in 1 ml of DDW. 50 µl of Folin & Ciocalteu's Phenol (FCP) reagent (~ 2N) were added to 100 µl each of the standard solution as well as in the Ag NPs. The mixture samples were made up to 1 ml and allowed to incubate at room temperature for 30 minutes. The association of TA in the particles was then determined by monitoring specific absorbance at 766 nm.

Antimicrobial activity assay via disc diffusion method

The tailored Ag NPs of different morphologies were subjected for their antimicrobial activity. In-vitro screenings of these particles were done by disc diffusion assay method against *Escherichia coli* (E. coli), taken as a model microbe. The disc diffusion method for antibiotic susceptibility testing is the Kirby-Bauer method. The freeze dried microbial mass was subjected for revival process as mentioned in guidelines given by MTCC. The microbial strains were then cultured in nutrient broth for preparing stock solution. This stock solution was kept at 37 °C in an incubation chamber for 24 hours previously before use.

Table 1. Culture medium for *E. coli* (gm/l).

Composition	Amount
Glucose	5gm
Na_2HPO_4	6gm
KH_2PO_4	3gm
NH_4Cl	1gm
NaCl	0.5gm
$MgSO_4$	0.12gm
$CaCl_2$	0.01gm
Agar-agar	2% by wt

For carrying out the antimicrobial assay against *E.coli*, synthetic medium was used. The stock solution of this media was prepared and sterilized by autoclaving it at for 15 minutes using pressure of 15 lb/sq. in. The culture media for the *E. coli* is presented in tabular form (**Table 1**).

All the glassware including micropipettes, pipette tips were also sterilized by autoclaving before used. Various concentrations of the forementioned morphologically unidentical Ag NPs i.e. (125 µg/ml, 250 µg/ml, 375 µg/ml and 500 µg/ml) were performed. This method is well documented and standard zones of inhibition have been estimated for susceptible and resistant values. Soon after the addition of nanodimensional Ag particles to the inoculated petri-plates, the plates were then kept for incubation at 37 °C for 24 hours and the zone of inhibitions were recorded afterwards.

Results and discussion

There has been a growing interest in biomimetic creation of nanoscale materials with complex morphology and controlled size in aqueous medium under ambient conditions. In this research work, we have successfully generated spherical and wire type nanodimensional Ag particles at room temperature using environmentally benign tannic TA as reducing agent. The synthesis methodology is presented as **Scheme 1**. Indeed preparation of particles was accomplished in a conventional manner, no sophisticated instruments and harsh conditions were employed.

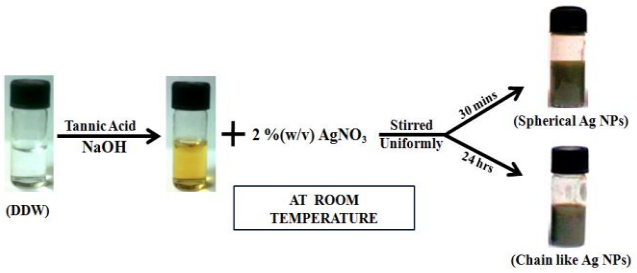

Scheme 1. Synthesis of nanosize Ag particles.

TA has been reported extensively for its antioxidant and chelating behavior for several inorganic cations **[4, 20]**. The role of hydroxyl groups accompanied with polyphenolic compounds in the formation of NPs was investigated earlier and results appear that the molecule should have at least two hydroxyl groups at the ortho or para positions to each other to undergo two-electron oxidation to the corresponding quinone form for facile reduction of metal ions **[21]**.

Even though, there are 25 phenolic OH groups present in TA only 10 pairs of o-dihydroxyphenyl groups are reported to be capable of taking part in redox reactions to form quinones and donate electrons, owing to the chelating action of adjacent hydroxyl groups and constraints on carbon valency **[22]**. Therefore, the hydroxyls of the phenolic groups present in the TA may be responsible for reducing Ag salt. Carboxylic acid groups (-COOH) accompanied in the TA lose their hydrogen atom to become carboxylate ion (COO−) during the reduction process. The (COO−) group so formed attaches to the surface of metal NPs along with the remaining part of the polymer to act as surfactant and stabilize the metal particles via electro steric interaction **[23]**. **Fig. 1** display the structure of TA and the probable reaction mechanism for the formation of Ag NPs utilizing TA can be represented as in **Fig. 2 [23, 24]**.

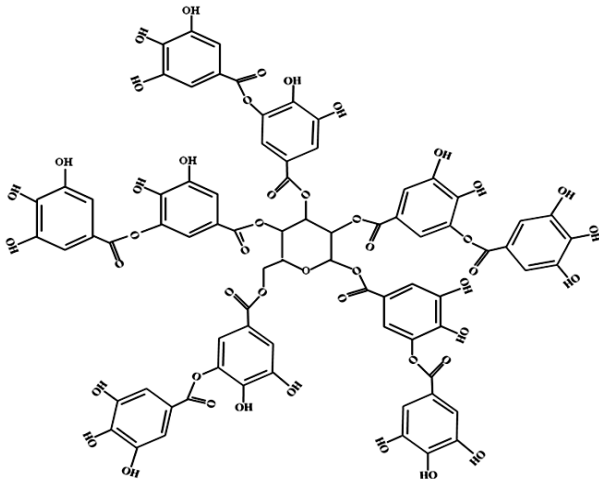

Fig. 1. Structure of tannic acid (C76H82O46).

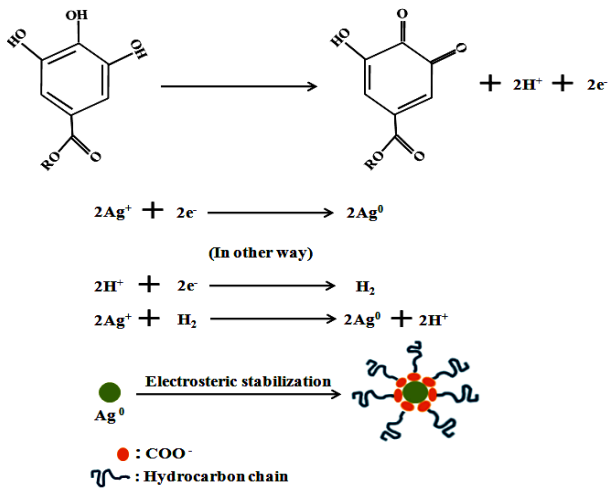

Fig. 2. Probable mechanism for the formation of Ag NPs.

Fig. 3 shows the UV–visible spectra of the synthesized Ag NPs and TA. The centrifuged particles exhibit well defined plasmon band at 474 nm and 482 nm, characteristic of nanosized Ag, for 30 minutes and 24 hours stirring respectively.

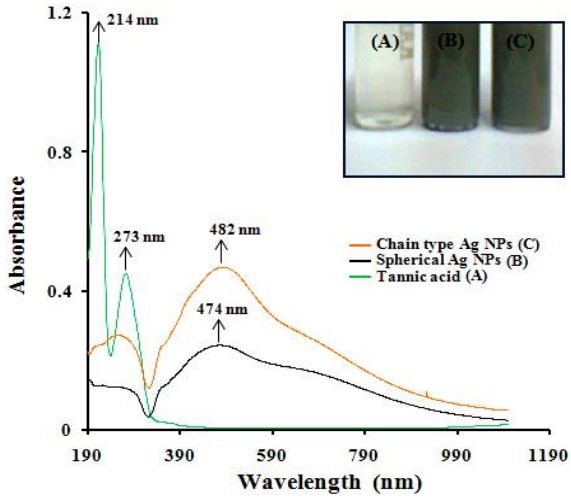

Fig. 3. UV-Visible absorption spectrum of (A) TA, (B) spherical and (C) chain type Ag NPs; inset shows their digital images.

The absorption spectrum of TA shows two distinct peaks at 214 nm and 273 nm. The absorption peak of TA at 273 nm is also observed in both the spectra of Ag NPs indicating the presence of TA along with the particles. During synthesis upon stirring the colour of both the solutions change and the particles remain stable for more than a week without settling down. Thus, TA acts as a good stabilizing agent. **Fig. 4** displays the typical TEM and SAED images of the Ag NPs. Nanoscale Ag particles initially obtained by stirring only for 30 minutes have an average diameter of 70 nm. The particles are spherical, crystalline and well monodispersed as can be seen from **Fig. 4(A)**. On the other hand, **Fig. 4(B)** presents the TEM images of Ag NPs generated by stirring for 24 hours under identical conditions. A closure inspection of these images show fusion among growing NPs from smaller spherical particles indicating the facilitation of Ostwald ripening process leading to the formation of super-structures **[25]**.

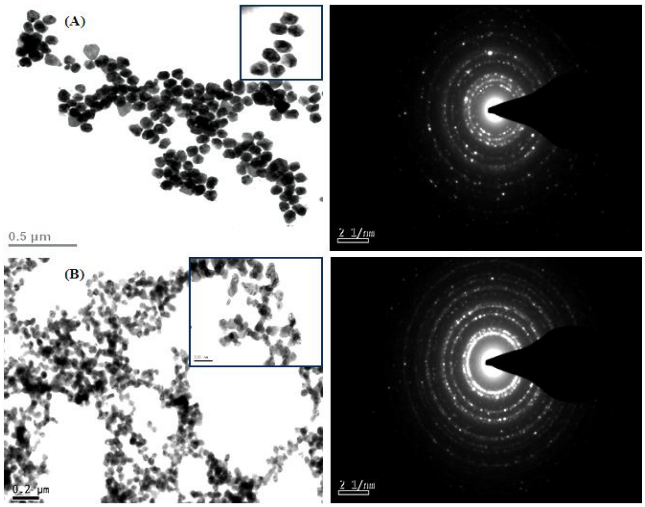

Fig. 4. TEM and SAED electron micrographs of (A) spherical and (B) chain type Ag NPs; insets show their respective HRTEM images.

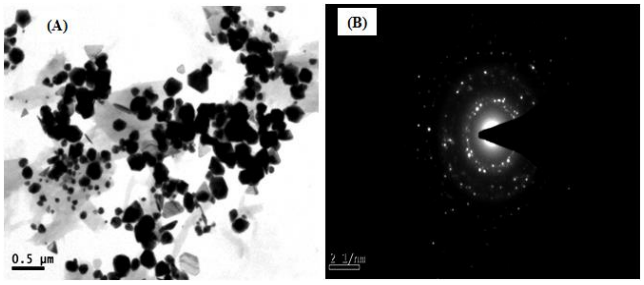

Fig. 5. (A) TEM and (B) SAED pattern of Ag NPs prepared in absence of NaOH.

The particles adopt elongated chain like structure linking individual particles with an average diameter of about 50 nm. Such nanosized chain type particles have also been reported earlier **[26-28]**. Although a precise formation mechanism is not established, we hypotheses that TA molecules may adsorb on different crystal plane of Ag nanocrystals lowering surface energy of their crystal lattice and selectively modifying their growth behaviour as noticed by Xuelin Tian *et al.* **[29]** and Stacey N Barnabey *et al.* **[27]** with ellagic acid. The nanochain Ag particles are also highly crystalline in nature as we observed from its SAED pattern. Moreover, Ag NPs can also be synthesized conveniently in absence of NaOH under the same condition as we have mention above unlike the observation made by Ioan Călinescu *et al.* **[30]**. However, the particles are not homogeneous and results in various types of irregular shapes in large intensity as we have seen via TEM image shown in **Fig. 5**.

The crystalline nature of the synthesized particles is also evident from their XRD data. The XRD patterns of the synthesized Ag NPs are shown in **Fig. 6**. In both the cases five well-defined characteristic diffraction peaks corresponding to the (111), (200), (220), (311) and (222) sets of lattice planes are observed consistent to SAED which may be indexed as the band for face centered cubic (fcc) structure of Ag NPs (JCPDS file no:-04-0783).

The peak corresponding to the (111) plane is more intense than the other planes. No impurities can be detected from these patterns which indicate that pure crystalline Ag particles are obtained under the present preparation conditions.

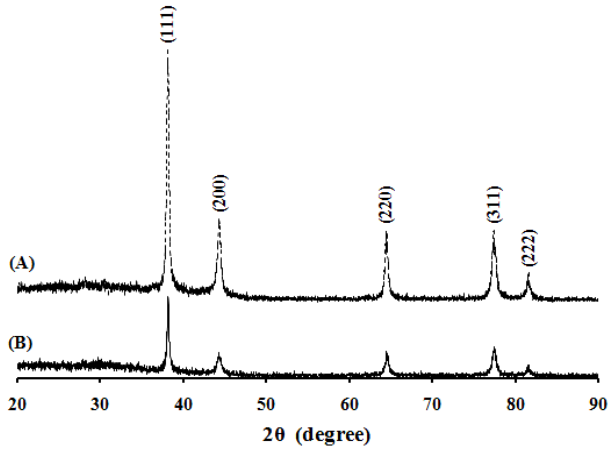

Fig. 6. XRD pattern of Ag NPs (A) spherical and (B) chain type.

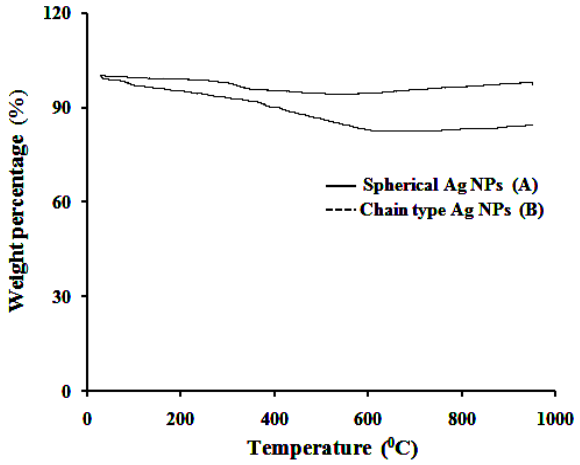

Fig. 7. TGA data of (A) spherical and (B) nanochain Ag particles.

TGA results of the TA stabilized Ag NPs obtained under nitrogen atmosphere are presented in **Fig. 7**. The thermogram shows a slow decrease in the weight of spherical Ag NPs unlike the chain type Ag particles where

a progressive loss of the weight occurs. This may be attributed to the decomposition of surface coated TA molecules as well as adsorbed water molecules upon increasing temperature.

The thermogram indicates about 3 % and 16 % loss in the weight of spherical and nanochain type Ag particles occur respectively at a temperature of 950 ^{o}C indicating thermal stability of the tailored particles over a wide range of temperature. Moreover, **Fig. 8** presents the FT-IR spectrum of TA and Ag NPs. The deformation vibration of the carbon-carbon bonds in the phenolic groups absorbs in the region of 1500-1400 cm^{-1}. At 755 cm^{-1} distortion vibration of C=C in benzene rings can be noticed vividly. Around 1449 cm^{-1} stretching vibrations of -C-C aromatic groups appear in spectrum. Moreover, the spectrum of TA indicates the inclusion of some aromatic esters due to the signal characteristics bands of carbonyl groups: C=O stretching vibration at 1730-1705 cm^{-1} and C - O at 1100-1300 cm^{-1} **[31]**.

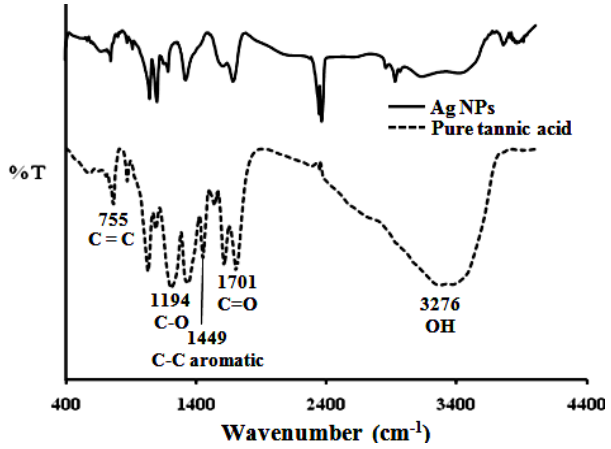

Fig. 8. FT-IR spectrum of pure TA and the tailored Ag NPs.

This FT-IR spectroscopic study investigates the plausible route behind the formation of these Ag NPs and offer information regarding the chemical change of the functional groups involved in reduction. The broad band in the region 3100-3400 cm^{-1} is due to OH stretching vibrational frequencies and due to the wide variety of hydrogen bonding between OH groups **[32]**.

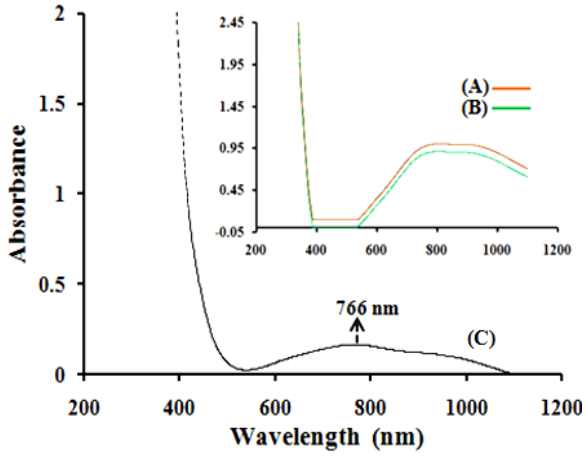

Fig. 9. Absorption spectra of (A) nanochain (B) spherical Ag particles and (C) pure TA in presence of FCP reagent.

Such intense strong band reveals the presence of organic molecules with alcohol functional groups. However, it may be observed that the intensity of this band decreases significantly in case of Ag NPs indicating the involvement of phenolic groups during the formation and stabilization of particles in conformity with our previous above synthetic mechanism. Prominent characteristic absorption peaks of TA are also observed in case of Ag NPs which provides a direct evidence for its association with the metal particles. The above argument is further supported by the qualitative estimation of TA via Folin-Ciocalteu method. FCP upon reacting with TA like molecules gives a blue coloured solution with a prominent peak at a wavelength of 766 nm, the intensity of which is proportional to the amount of TA **[33, 34]**. From **Fig. 9**, it can be noticed that such characteristic peak of the product is also observed in case of the synthesized nanoscale Ag particles coated with TA even though the peaks monitor in these cases are slightly broad as compared to the free TA solution.

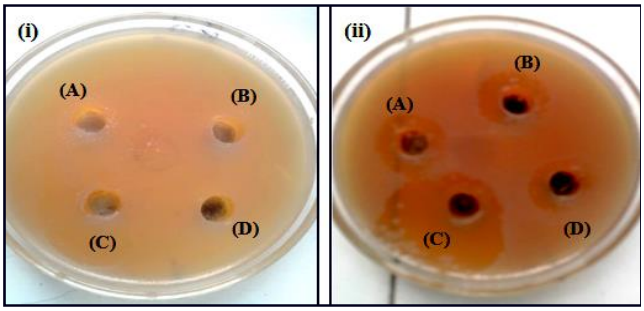

Fig. 10. Zone of inhibition of *E.coli* in presence of Ag NPs (i) spherical and (ii) chain type.

Nano dimensional Ag particles with their unique chemical and physical properties provide an alternative for the development of new antibacterial agents. There is a necessity of drawing attention regarding the structural and functional changes induced by metal nanostructures in the organization of the bacterial cell. Earlier it has been reported that TA doesn't exhibit anti-bacterial activity on *E. coli* **[10]**, so in this particular study the authors omit control evaluation of antibacterial activity with TA instead focus on morphological behaviour of NPs. The bactericidal effects of the synthesized nanocrystalline Ag particles of different concentrations were examined against *E. coli* strain by disc diffusion method as displayed in **Fig. 10**.

The inhibition zone diameter were calculated and plotted against the concentration of Ag NPs as shown in **Fig. 11**. Spherical Ag NPs possess higher anti-bacterial property as compared to the nanochain type Ag particles and as the concentration of the particles increase their anti-bacterial property rise.

However, for chain type Ag NPs the increase in antibacterial property decrease slightly after the third reading. The higher anti-bacterial behaviour of spherical Ag NPs may be because of its larger surface to volume ratio than the nanochain Ag particles. As the results show, the spherical NPs have stronger antibacterial property than that of the nanochain type ones at the same concentration of Ag particles and even at different size. However, the mechanism of nanosize Ag particles acting as biocidal

material against bacteria is still not well understood. We speculate that Ag NPs must have interacted with the bacterial cell wall and get accumulated at the cell membrane causing major damage such as formation of pits in them. While some of the particles successfully penetrated into the cells. Such pitting leads to an increase in permeability and oozing out of intracellular materials. These cause significant changes to the cell structure and eventually originate to cell death as we have noticed via electron microscope. A graphical presentation of probable antibacterial mechanism of Ag NPs on E.coli is provided in **Fig. 12**.

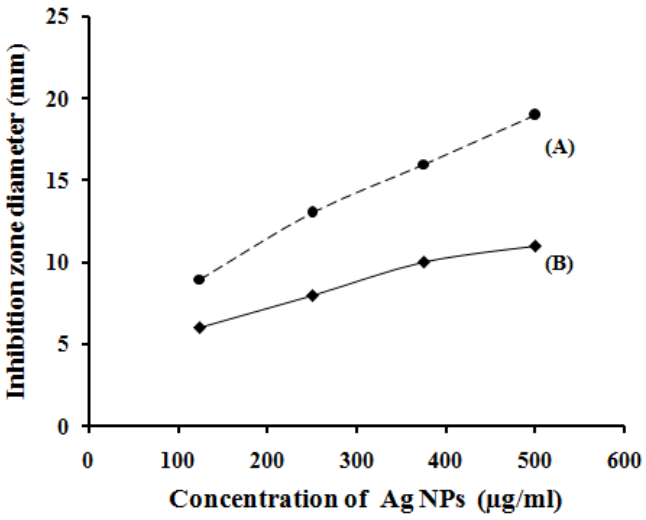

Fig. 11. Plot of zone of inhibition of E.coli as a function of the concentration of (A) spherical and (B) chain type nanosized Ag particles.

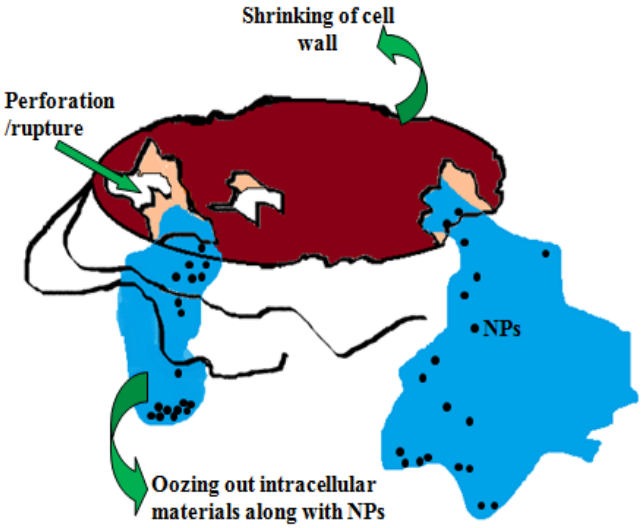

Fig. 12. Pictorial representation of antibacterial mechanism of nanosized Ag particles.

However, this observation is crucial for explaining the antibacterial mode of these particles as there are earlier reports available in the literature regarding the metal ions uptake (translocation and particle internalization) into cells followed by depletion of intracellular ATP production and disruption of DNA replication as well as generation of ROS (reactive oxygen species) from metal NPs and metal ions, with subsequent oxidative damage to cellular structures **[35-38]**. This report may assist in explaining anti-bacterial behavior of metal NPs and confirmed that nanosized Ag particles of different morphologies exhibit antimicrobial activity to different extend revealing that they represent a useful target for future application of novel antimicrobial compounds. Therefore, it can be anticipated that such antibacterial nanomaterial may be used in some potential antibacterial biomedical applications such as wound healing, infections and in antibacterial ultrafiltration membranes used for water treatment **[39, 40]**. It is inexorable that nanoscale materials will make their path in the commercial market. Increase in utilization and dispose of such particles as waste in the surrounding natural environment should be carefully regulated.

Conclusion

We have demonstrated a simple, versatile, cost effective and eco-friendly single-step green chemistry approach for the fabrication of spherical and chain type Ag NPs at room temperature utilizing TA as both reducing and stabilizing agent. Most of these green aqueous techniques are still in the development stage and the problems counter are stability, control of crystal growth, morphology and size distribution. This report will enable rational development of biomaterials based synthesis procedure for other metal nanomaterials also. The synthesized particles are monodispersed with 70 nm and 50 nm as average diameter for the spherical and the chain type Ag particles. The plausible formation mechanism of Ag NPs and shape evolution of chain type observed in present work has been successfully explained. The tailored nanoscale Ag particles of different morphologies exert significant antibacterial properties against multidrug resistant gram-negative E.coli. However, spherical Ag NPs exhibit stronger antibacterial behaviour as compare to the nanochain Ag particles in spite of its larger size indicating that antibacterial activity of particles depend on their morphology. This environmentally friendly and less sophisticated technique may represent as an alternative to the existing methods for the production of large-scale Ag NPs of varied morphology that can be employed in electronics, sensor, catalysis and biomedical applications.

Acknowledgements

The authors are thankful to AIIM, Delhi and USIC, University of Delhi, for allowing us to utilize the necessary instrumentation facilities. We are also grateful to University Grant Commission, Government of India, for providing us financial assistance in the form of a research project. H.P. Singh is also thankful to CSIR, Delhi, India for its support in the form of SRF award.

Reference

1. Perro, A.; Reculusa, S.; Ravaine, S.; Lamic, E, B.; Duguet, E. *J. Mater. Chem.*, **2005**, *15*, 3745. **DOI:** 10.1039/b505099e
2. Gubicza, J.; Lábár, J. L.; Quynh, L. M.; Namc, N. H.; Luong, N. H.; *Mater. Chem. and Phys*., **2013**, *138*, 449. **DOI:** 10.1016/j.matchemphys.2013.01.012
3. Salam, H. A.; Rajiv, P.; Kamaraj, M.; Jagadeeswaran, P.; Gunalan, S.; Sivaraj, R. I.; *Res. J. Biological Sci.*, **2012**, *1*, 85.
4. Yi, Z.; Li, X.; Xua, X.; Luo, B.; Luo, J.; Wu, W.; Yia, Y.; Tang, Y. *Colloids and Surf. A: Physicochem. Eng. Aspects*, **2011**, *392*, 131. **DOI:** 10.1016/j.colsurfa.2011.09.045

5. Chen, H, M.; Hsin, C. F.; Liu, R. S.; Lee, J. F.; Jang, L. Y.; *J. Phys. Chem. C.*, **2007**, *111*, 5909. **DOI:** 10.1021/jp070232l
6. Sathishkumar, M.; Sneha, K.; Won, S. W.; Cho, C. W.; Kim, S.; Yun, Y. S. *Colloids and Surf. B: Biointerf.*, **2009**, *73*, 332. **DOI:** 10.1016/j.colsurfb.2009.06.005
7. Dubey, S. P.; Dwivedi, A. D.; Lahtinen, M.; Lee, C.; Kwon, Y. N.; Sillanpa, M.; *Spectrochimica Acta Part A: Molecular and Biomolecular Spectroscopy*, **2013,** *103*, 134. **DOI:** 10.1016/j.saa.2012.11.021
8. Raghunandan, D.; Ravishankar, B.; Sharanbasava, G.; Mahesh, D. B.; Harsoor, V.; Yalagatti, M. S.; Bhagawanraju, M.; Venkataraman, A.; *Cancer Nano*, **2011,** *2*, 57. **DOI:** 10.1007/s12645-011-0014-8
9. Bhat, R.; Sharanabasava, V. G.; Deshpande, R.; Shetti, U.; Sanjeev, G.; Venkataraman, A.; *J. Photochemistry and Photobiology B: Biology* **2013**, *125*, 63. **DOI:** 10.1016/j.jphotobiol.2013.05.002
10. Gupta, N.; Panwa, A.; Kumar, R.; Sharma, S. K.; Sharma, R. K.; Agrawal, V.; *Adv. Sci. Eng. Med.* **2012**, *5*, 1. **DOI:** 10.1166/asem.2012.1264
11. Patel, D.; Patel, M.; Krishnamurthy, R.; *Cibtech J. Bio-Protocols* **2013**, *2*, 50.
12. Orr, G.; Panther, D. J.; Phillips, J, L.; Tarasevich, B, J; Dohnalkova, A.; Hu, D.; Teeguarden, J, G.; Pounds, J. G.; *ACS Nano*, **2007**, *1*, 463. **DOI:** 10.1021/nn700149r
13. Zhou, H.; Lee, J.; *Acta Biomaterialia*, **2011**, *7*, 2769. **DOI:** 10.1016/j.actbio.2011.03.019
14. Panacek, A.; Kvitek, L.; Prucek, R.; Kolar, M.; Vecerova, R.; Pizurova, N.; Sharma, V. K.; Neveena, T.; Zboril, R.; *J. Phys.Chem. B*, **2006**, *110*, 16248. **DOI:** 10.1021/jp063826h
15. Santos, C. A. D.; Jozala, A. F.; Pessoa Jr. A.; Seckler, M. M.; *J. Nanobiotechnology*, **2012**, *10*, 43. **DOI:** 10.1186/1477-3155-10-43
16. Pal, S.; Tak, Y. K.; Song, J. M.; *Applied and environmental microbiology*, **2007**, *73*, 1712. **DOI:** 10.1128/AEM.02218-06
17. Rai, M.; Yadav, A.; Gade, A.; *Biotechnology Advances*, **2009**, *27*, 76. **DOI:** 10.1016/j.biotechadv.2008.09.002
18. Antony, J. J.; Sivalingam, P.; Siva, D.; Kamalakkannan, S.; Anbarasu, K.; Sukirtha, R.; Krishnan, M.; Achiraman, S. *Colloids and Surf. B: Biointerf.* **2011**, *88*, 134. **DOI:** 10.1016/j.colsurfb.2011.06.022
19. Morones, J, R.; Elechiguerra, J. L.; Camacho, A.; Holt, k.; Kouri, J. B.; Ram´ırez, J, T.; Yacaman, M. J.; *Nanotech*., **2005**, *16*, 2346. **DOI:** 10.1088/0957-4484/16/10/059
20. Wei, D. W.; Qian, W. P.; Facile synthesis of Ag and Au nanoparticles utilizing chitosan as a mediator agent, Colloids Surf. B: Biointerf., **2008**, *2*, 136. **DOI:** 10.1016/j.colsurfb.2007.09.030
21. Yoosaf, K.; Ipe, B. I.; Suresh, C. H.; Thomas, K. G.; *J. Phys. Chem. C*., **2007**, *111*, 12839. **DOI:** 10.1021/jp073923q
22. Sivaraman, S. K.; Elango, I.; Kumar, S.; Santhanam, V.; *Current Sci*., **2009**, *97*, 1055.
23. Ahmad, T.; *J. Nanotech*., **2014**. **DOI:** 10.1155/2014/954206
24. Rao, K. J.; Paria, S.; *Mater. Res. Bull*., **2013**, *8*, 628. **DOI:** 10.1016/j.materresbull.2012.11.035
25. Rafiuddin, Z. Z.; *Colloids and surf. A: Physicochem. Eng.Aspects* **2012**, *393*, 1. **DOI:** 10.1016/j.colsurfa.2011.08.018
26. Han, X.; Goebl, J.; Lu, Z.; Yin, Y.; *Langmuir*, **2011**, *27*, 5282. **DOI:** 10.1021/la200459t
27. Barnaby, S. N.; Yu, S. M.; Fath, K. R.; Tsiola, A.; Khalpari, O.; Banerjee, I. A.; *Nanotech.*, **2011,** *22*, 225605. **DOI:** 10.1088/0957-4484/22/22/225605
28. Chirea, M.; Freitas, A.; Vasile, B. S.; Ghitulica, C.; Pereira, C. M.; Silva, F.; *Langmuir*, **2011**, *27*, 3906. **DOI:** 10.1021/la104092b
29. Tian, X.; Li, J.; Pan, S. J., *Nanopart. Res*., **2009**, *11*, 1839. **DOI:** 10.1007/s11051-009-9700-4
30. Calinescu, I.; Patrascu, M.; Gavrila, A. I.; Trifan, A.; Boscornea, C. U.P.B.; *Sci. Bull. Series B*., **2011**, *73*, 3.
31. Pantoja-Castro, M. A.; Rodrígueza, H. G.; *Rev. Latinoamer. Quím*., **2011,** *39*, 107.
32. Varshneya, R.; Bhadauria, S.; Gaur, M. S.; *Adv. Mat. Lett*., **2010**, *1*, 232. **DOI:** 10.5185/amlett.2010.9155
33. Blainski, A.; Lopes, G. C.; de Mello, J. C. P.; *Molecules*, **2013**, *18*, 6852. **DOI:** 10.3390/molecules18066852
34. Box, J. D., *Water Res*., **1983**, *17*, 511. **DOI:**10.1016/0043-1354(83)90111-2
35. Xiu, Z. M.; bo Zhang, Q.; Puppala, H. L.; Colvin, V. L.; Alvarez, P. J. J.; *Nano Lett*., **2012**, *12*, 4271. **DOI:** 10.1021/nl301934w
36. Jaidev, L. R.; Narasimha, G.; *Colloids and Surf. B: Biointerf*., **2010**, *81*, 430. **DOI:** 10.1016/j.colsurfb.2010.07.033
37. Sondi,I.; Sondi, B. S.; *J. Colloid and Interf. Sci.*, **2004**, *275*, 177. **DOI:** 10.1016/j.jcis.2004.02.012
38. Prabhu, S.; Poulose, E. K.; *Inter. Nano Lett.*, **2012**, *2*, 32. **DOI:** 10.1186/2228-5326-2-32
39. Mauter, M. S.; Wang, Y.; Okemgbo, K. C.; Osuji, C. O.; Giannelis, E. P.; Elimelech, M.; *ACS Appl. Mater. Interf.*, **2011**, *3*, 2861. **DOI:** 10.1021/am200522v
40. Lok, C. N.; Ho, C. M.; Chen, R.; He, Q. Y.; Yu, W. Y.; Sun, H.; Tam, P. K. H.; Chiu, J. F.; Che, C. M.; *J. Proteome Res*., **2006**, *5*, 916. **DOI:** 10.1021/pr0504079

